

# Medical Image Segmentation via Coupled Curve Evolution Equations with Global Constraints \*

Anthony Yezzi, Jr.

School of Electrical and Computer Engineering  
Georgia Institute of Technology  
Atlanta, GA 30332-0250

Andy Tsai Alan Willsky

Department of Electrical Engineering and Computer Science  
Massachusetts Institute of Technology  
Cambridge, MA 02139

## Abstract

*In this work we modify the coupled curve evolution approach to snakes presented by the authors in previous work for bimodal and trimodal imagery through the introduction of global constraints. The key idea, as before, is to derive curve evolution equations which “pull apart” the values of one or more statistics within the image. However, by imposing a new constraint on the evolution of these statistics, we are able to segment a larger class of medical imagery for which our original model would fail.*

## 1 Introduction

In [10, 11], the authors outlined a fully global, coupled curve evolution approach to image segmentation for images consisting of a known number of regions distinguishable by a given set of statistics. This work, along with the recent work in [2, 7], enjoyed widespread success by many region-based approaches to snakes [1, 7, 8, 12] of being less sensitive to noise than most edge-based approaches by avoiding differential operators to detect edges in the image. Such approaches gain yet another degree of robustness by being less local than typical edge-based approaches.

In contrast to other region-based snake algorithms, the technique in [10, 11] employs an independent set of curves for each region-type to be captured in the image. This facilitates the level set implementation (see Osher and Sethian [6, 9] and the references therein) used by the authors by allowing a separate level set

function for each evolving curve.<sup>1</sup> The separate curve evolution equations are coupled via a common energy functional yielding a fully global model for segmentation in which the evolution of each curve, regardless of its proximity to any other curve, depends upon statistics computed within every other curve and thereby involves every single pixel in the image. The basic idea behind the original technique was to design these curve evolution equations to maximally separate two or more values of a predetermined set of statistics within the image data.

In many medical images, mean intensity values constitute an adequate statistic to distinguish one region type from another. However, a maximal separation of the mean intensities does not always correspond with the desired segmentation. Even in bimodal images involving a dark tissue and a light tissue, a slight inhomogeneity in one of the tissues could generate a particularly bright (or dark) spot within the image which could attract an evolving curve more powerfully than the actual boundary between the two tissues. It is precisely this situation that motivates the work in this paper. We add the constraint that the evolving curves must not only separate the statistics within each region but must also force each individual statistic to move away from all other statistics.

This paper is organized as follows. We first describe the original curve evolution model proposed in [10, 11] for bimodal and trimodal images. We then present a medical image for which the original algorithm was expected to perform well but did not. The

---

\*This work was supported by ONR grant N00014-91-J-1004, by subcontract GC123919NGD from Boston University under the AF OSR Multidisciplinary Research Program on Reduced Signature Target Recognition, and by ARO grant DAAH04-96-1-0494 through Washington University.

---

<sup>1</sup>Note that Chan and Vese [2] and Paragios and Deriche [7] also utilize level set implementations but only with a single level set function.

remainder of the paper explains the unexpected failure of the original algorithm and outlines the implementation of a new global constraint on the evolution of the statistics within each evolving curve which remedies the poor performance of the original algorithm on this and other related medical images.

## 2 Coupled Curve Evolution Models

In this section, we present gradient flows designed to segment images consisting of a known number of regions. These flows will be constructed to essentially “pull-apart” the values of a given set of statistics as far as the data in the image will allow. For a more thorough treatment, we refer the interested reader to [10, 11].

### 2.1 Binary Flows

We begin by considering images which consist of just two region types. The most trivial case is that of a binary image  $I(x, y)$  consisting of a single foreground region  $R$  of intensity  $I^r$  and a complementary background region  $R^c$  of intensity  $I^c \neq I^r$ . We wish to determine an evolution that will continuously attract any initial closed curve  $\vec{C}$  toward the boundary  $\partial R$  of  $R$ . Given that  $\vec{C}$  will enclose some portion of  $R$  and some portion of  $R^c$ , the average intensities  $u$  and  $v$  inside and outside the curve, respectively, will be bounded above and below by  $I^r$  and  $I^c$ . Consequently, using the distance between  $u$  and  $v$  to measure how well  $\vec{C}$  has separated the foreground from the background will ensure an upper-bound of  $|I^r - I^c|$  that is uniquely attained when  $\vec{C} = \partial R$ . A similar strategy, which also assumes no previous knowledge of  $I^r$  or  $I^c$ , would be to descend along the following quadratic energy functional:

$$E = -\frac{1}{2}(u - v)^2. \quad (1)$$

Let  $S_u = \int_{R^u} I dA$  and  $A_u = \int_{R^u} dA$ , where  $R^u$  denotes the interior of  $\vec{C}$ . By expressing their first variations as  $\nabla S_u = I \vec{N}$  and  $\nabla A_u = \vec{N}$  (see [10] for details), where  $\vec{N}$  denotes the outward unit normal of  $\vec{C}$ , we compute the first variation of  $u = S_u/A_u$  as

$$\nabla u = \frac{A_u \nabla S_u - S_u \nabla A_u}{A_u^2} = \frac{I - u}{A_u} \vec{N}. \quad (2)$$

Using this expression (and a similar expression for  $\nabla v$ ), we compute the gradient flow for  $\vec{C}$  as

$$\frac{d\vec{C}}{dt} = -\nabla E = (u - v) \left( \frac{I - u}{A_u} + \frac{I - v}{A_v} \right) \vec{N}, \quad (3)$$

yielding an evolution that pulls apart the mean intensities inside and outside the curve as fast as possible.

In a more general bimodal image which contains noise, a contour may tend to weave around or encircle extremely small regions due to noise in order to fully separate the interior and exterior means, causing the contour to appear fractal. To counter such effects, we follow the lead of Mumford and Shah [5] by adding to our functional (1) a penalty on the arclength of the curve.

$$E = -\frac{1}{2}(u - v)^2 + \alpha \int_{\vec{C}} ds \quad (4)$$

Incorporating such a geometric constraint has the effect of regularizing the evolution through a curvature-dependent term in the resulting gradient flow equation

$$\frac{d\vec{C}}{dt} = (u - v) \left( \frac{I - u}{A_u} + \frac{I - v}{A_v} \right) \vec{N} - \alpha \kappa \vec{N}. \quad (5)$$

This additional term exerts its strongest influence at points on the contour where the magnitude of the curvature is large. This discourages the contour from wrapping around tiny pieces of noise, with the tradeoff that sharp corners in the image data may be rounded off by the final contour.

One can, of course consider separating statistics other than mean intensities. Furthermore, even with just two regions, it is not necessary to employ just a single statistic at a time. We may generalize our binary model by considering the following more general energy functional:

$$E = -\frac{1}{2} \|u - v\|^2 + \alpha \int_{\vec{C}} ds, \quad (6)$$

where  $u = (u_1, \dots, u_n)$  and  $v = (v_1, \dots, v_n)$  now denote vectors of statistics inside and outside the curve, respectively. The basic idea is to determine a set of statistics which distinguish the one region from another and then utilize the following curve evolution equation to “pull the statistics apart,”

$$\frac{d\vec{C}}{dt} = \sum_{i=1}^n (u_i - v_i) (\nabla u_i - \nabla v_i) - \alpha \kappa \vec{N} \quad (7)$$

where  $\nabla u_i$  and  $\nabla v_i$  denote the first variations of  $u_i$  and  $v_i$ , respectively. To accommodate a larger class of bimodal imagery, the statistics  $u_i$  and  $v_i$  do not necessarily have to represent mean intensities but may represent variances, correlations between wavelet coefficients, and a variety of other statistics. However, we have found that for a large class of medical imagery, mean intensities work quite effectively.

## 2.2 Ternary Flows

We now consider trimodal imagery (three region types instead of just two) by assuming that the domain of an image  $I(x, y)$  consists of two disjoint, simply connected, foreground regions  $R^a$  and  $R^b$ , and a background region  $R^c$  (the complement of  $R^a \cup R^b$ ) with mutually distinct intensities  $I^a$ ,  $I^b$ , and  $I^c$ , respectively. A closed curve  $\vec{C}_u$  in the domain of  $I$  will generally enclose some portion of each region; thus, the average intensity inside  $\vec{C}_u$  can be written as a convex combination of  $I^a$ ,  $I^b$ ,  $I^c$  (i.e.  $u = \alpha I^a + \beta I^b + \gamma I^c$  where  $0 \leq \alpha, \beta, \gamma \leq 1$  and  $\alpha + \beta + \gamma = 1$ ). Unfortunately, if  $I$  takes its values in  $\mathbf{R}$ , there is no unique convex combination since any three points in  $\mathbf{R}$  are obviously collinear. This poses a problem since the algorithm we are about to present relies upon geometrically independent<sup>2</sup> statistics to distinguish the regions  $R^a$ ,  $R^b$ , and  $R^c$ .

To be geometrically independent,  $I^a$ ,  $I^b$ , and  $I^c$  must belong to  $\mathbf{R}^n$  where  $n \geq 2$  as opposed to just  $\mathbf{R}$ . For this reason, assume that  $I$  is a vector-valued image with vectors in  $\mathbf{R}^n$  ( $n \geq 2$ ) and that  $I^a, I^b, I^c$  are geometrically independent. We may now represent  $u$  as a unique convex combination of these three values. The same situation applies to the average intensity  $v \in \mathbf{R}^n$  within the interior of a second curve  $\vec{C}_v$  and to the average intensity  $w \in \mathbf{R}^n$  within the mutual exterior of  $\vec{C}_u$  and  $\vec{C}_v$ . Our segmentation goal is to construct coupled flows that will continuously attract  $\vec{C}_u$  towards one of the boundaries  $\partial R^a$  or  $\partial R^b$  (of  $R^a$  and  $R^b$ , respectively) while simultaneously attracting  $\vec{C}_v$  towards the other.

By virtue of their geometric independence,  $I^a$ ,  $I^b$ , and  $I^c$  form the vertices of a triangle  $T_{abc}$ . As convex combinations of these three values,  $u$ ,  $v$ , and  $w$  lie within this triangle, forming another triangle  $T_{uvw}$  completely contained in  $T_{abc}$ . This is true even if the interiors of  $\vec{C}_u$  and  $\vec{C}_v$  overlap (providing a flexibility to our approach that is not provided by other region-based approaches in which evolving regions must always be disjoint). As such, the area of the triangle  $T_{uvw}$  will always be less than or equal to the area of the triangle  $T_{abc}$ , with equality holding if and only if  $\vec{C}_u = \partial R^a$  and  $\vec{C}_v = \partial R^b$  or vice-versa. We may therefore attract  $\vec{C}_u$  and  $\vec{C}_v$  toward the desired boundaries without any prior knowledge of  $I^a$ ,  $I^b$ , or  $I^c$  by trying to maximize the area of  $T_{uvw}$  using the following expressions:

$$\text{area}(T_{uvw}) = \frac{1}{2} \|u - w\| \|v - w\| \sin \theta$$

$$4 \text{ area}^2(T_{uvw}) = \|u - w\|^2 \|v - w\|^2 - ((u - w) \cdot (v - w))^2$$

<sup>2</sup>Noncollinear in this context.

where  $\theta$  denotes the angle between  $u - w$  and  $v - w$ .

As in Section 2.1 we also attach a penalty on the arclengths of  $\vec{C}_u$  and  $\vec{C}_v$  to regularize the evolutions and prevent the final contours from capturing small pieces of noise. In general one may wish to penalize the two lengths differently; here we consider an equal penalty to obtain the following energy functional

$$E = -2 \text{ area}^2(T_{uvw}) + \alpha \left( \int_{\vec{C}_u} ds + \int_{\vec{C}_v} ds \right) \quad (8)$$

where  $\alpha \geq 0$ . Using the previous expressions to compute the variation of the first term yields

$$\nabla(2 \text{ area}^2(T_{uvw})) = \{\bar{w} \cdot \nabla u + \bar{u} \cdot \nabla v + \bar{v} \cdot \nabla w\} \vec{N}$$

with the following definitions:

$$\nabla u = (\nabla u_1 \cdot \vec{N}, \dots, \nabla u_n \cdot \vec{N})$$

(likewise for  $\nabla v$  and  $\nabla w$ )

$$\begin{aligned} \bar{u} &= \hat{u} - \hat{v}, & \hat{u} &= \hat{u}(\hat{v} \cdot \hat{u}), & \hat{u} &= u - v \\ \bar{v} &= \hat{v} - \hat{w}, & \hat{v} &= \hat{v}(\hat{w} \cdot \hat{v}), & \hat{v} &= v - w \\ \bar{w} &= \hat{w} - \hat{u}, & \hat{w} &= \hat{w}(\hat{u} \cdot \hat{w}), & \hat{w} &= w - u. \end{aligned}$$

Since  $\nabla_{\vec{C}_u} v = \nabla_{\vec{C}_v} u = 0$  the gradient descent equations for  $E$  become

$$\frac{d\vec{C}_u}{dt} = \left\{ \sum_{i=1}^n \left( \bar{w}_i \frac{I_i - u_i}{A_u} - \bar{v}_i (1 - \chi_v) \frac{I_i - w_i}{A_w} \right) - \alpha \kappa_u \right\} \vec{N}_u \quad (9)$$

$$\frac{d\vec{C}_v}{dt} = \left\{ \sum_{i=1}^n \left( \bar{u}_i \frac{I_i - v_i}{A_v} - \bar{w}_i (1 - \chi_u) \frac{I_i - w_i}{A_w} \right) - \alpha \kappa_v \right\} \vec{N}_v \quad (10)$$

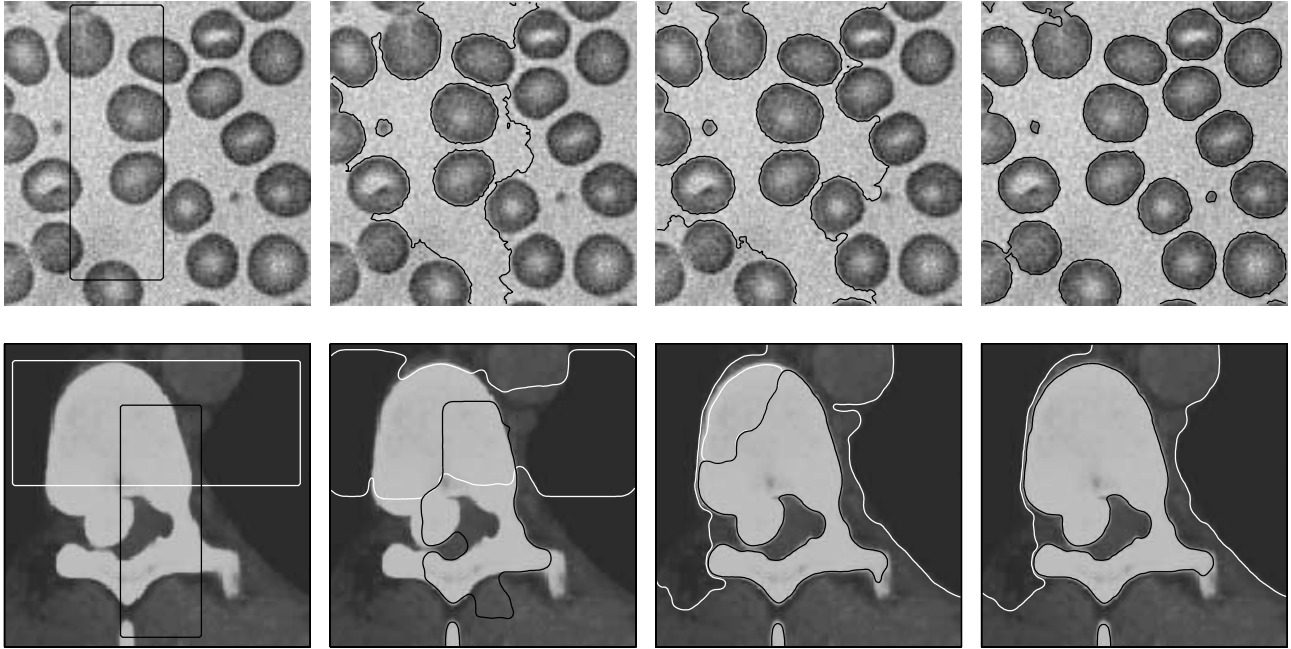
where  $\kappa_u$  and  $\kappa_v$  denote the signed curvatures of  $\vec{C}_u$  and  $\vec{C}_v$ ,  $\vec{N}_u$  and  $\vec{N}_v$  denote their outward unit normals, and  $\chi_u$  and  $\chi_v$  denote the characteristic functions over  $R^u$  and  $R^v$  (the interiors of  $\vec{C}_u$  and  $\vec{C}_v$  respectively).

Note that equations (9) and (10) comprise a truly global model for segmentation in that the evolutions of  $\vec{C}_u$  and  $\vec{C}_v$  are always coupled (through the statistics  $u$ ,  $v$ , and  $w$ ), regardless of their proximities to one another. As a consequence the evolution of each curve is governed by the value of every single pixel in the image at all times.

## 2.3 More general coupled flows

In general, one may wish to partition an image domain into  $m$  different types of regions, where  $m$  is an arbitrarily large number. By adhering to the same philosophy of associating the preferred segmentation with a maximal separation of some statistic over each region, a vector-valued statistic  $U$ , with at least  $m - 1$  components would be required. If the  $m$  distinct values,  $U^1, \dots, U^m$ , of this statistic constitute a set of

Figure 1: Original binary (top) and ternary (bottom) flows segmenting red blood cells and a dorsal spine.



geometrically independent points in the preferred segmentation, and if the statistic is chosen such that an arbitrary segmentation yields values  $u^1, \dots, u^m$ , which are convex combinations of  $U^1, \dots, U^m$  (which is the case if we are considering means of a vector-valued image) then the natural energy functional will relate to the volume of the  $m - 1$  dimensional simplex whose vertices are given by  $u^1, \dots, u^m$ . The corresponding gradient flow equations will yield a coupled evolution of  $m - 1$  curves which tend to maximize the volume of this simplex, with the interiors of each curve representing  $m - 1$  regions and their mutual exteriors representing the  $m$ 'th region.

### 3 Global Constraints

We begin this section by illustrating the performance of our coupled curve evolution models on three medical images. The two rows in Fig. 1 demonstrate successful uses of the binary flow (5) and the coupled ternary flows (9) and (10) respectively to segment a bimodal microscopic image of red blood cells and a trimodal CT image of the dorsal region of a spine (using pseudocolor to generate a vector-valued image). In the first row of Fig. 2 we see a cardiac ultrasound image of the left ventricle which, like the first image in Fig. 1, consists of light and dark regions and is therefore bimodal in nature. In this case, however, the same binary flow fails to capture the boundary between these

two regions but captures instead the very dark spot within the blood pool.

The undesirable behavior of the binary flow (5) in Fig. 2 (first row) may be explained by noting that both means (inside and outside the curve) decrease as the curve moves past the ventricle boundary and into the blood pool. However, the rapid decrease of the interior mean outweighs the slow decrease in the exterior mean so that overall, the two means move further apart, just as the binary model dictates. This observation suggests imposing a constraint on the evolution of the two means: Not only do we desire the means to move further apart, we also require that they always move in opposite directions. We now develop an implementation of this constraint to obtain a binary flow which pulls two means apart as fast as possible without allowing them to evolve in the same direction.

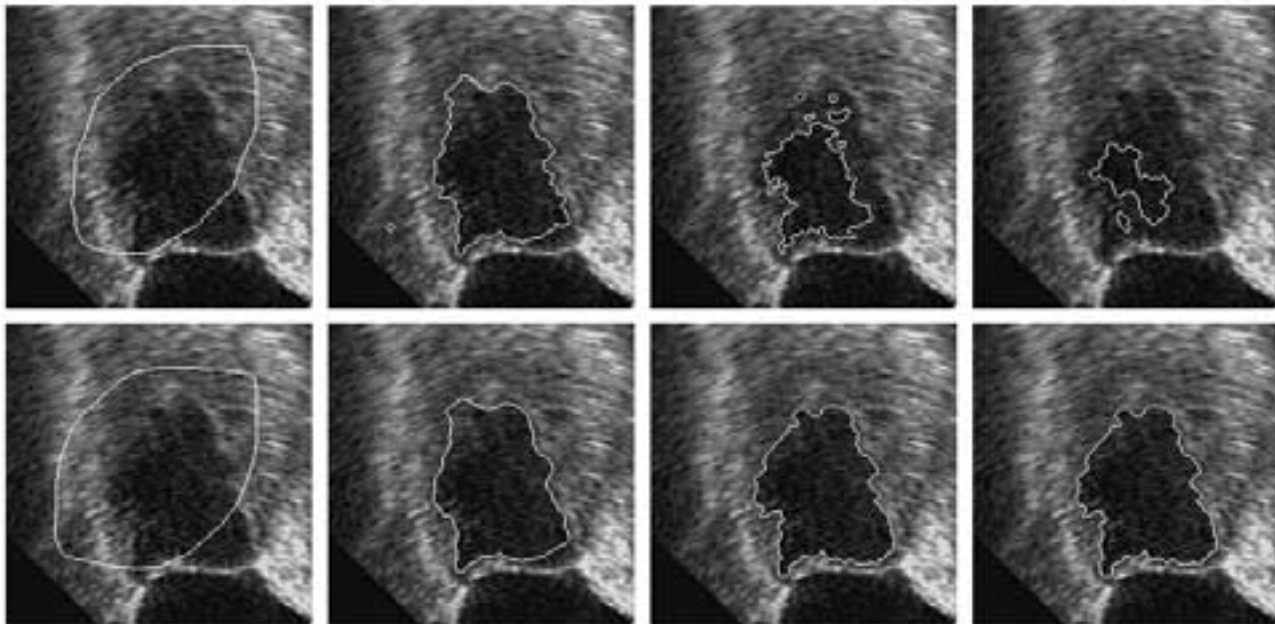
#### 3.1 Constrained binary flows

Let  $\frac{d\vec{C}}{dt}$  and  $\frac{d\vec{C}'}{dt}$  denote two evolutions taken from the space of all smooth evolutions of a curve  $\vec{C}$ . We may obtain the structure of a Hilbert space by defining the following inner product.

$$\left\langle \frac{d\vec{C}}{dt}, \frac{d\vec{C}'}{dt} \right\rangle = \oint_{\vec{C}} \left( \frac{d\vec{C}}{dt} \cdot \frac{d\vec{C}'}{dt} \right) ds \quad (11)$$

Returning to our original binary energy functional (1), we denote its gradient (descent) flow (3) by  $-\nabla E$

Figure 2: The constrained binary flow (bottom) outperforming the original binary flow (top).



and we denote the gradient flows<sup>3</sup> for the means  $u$  and  $v$  by  $\nabla u$  and  $\nabla v$  respectively. Under the binary flow  $-\nabla E$  the means  $u$  and  $v$  evolve according to

$$u' = \langle \nabla u, -\nabla E \rangle = (u - v)(\Gamma(u, u) - \Gamma(u, v)) \quad (12)$$

$$v' = \langle \nabla v, -\nabla E \rangle = (u - v)(\Gamma(v, u) - \Gamma(v, v)) \quad (13)$$

where  $\Gamma(u, v)$  denotes the inner product  $\langle \nabla u, \nabla v \rangle$ . In this case, since  $u$  and  $v$  denote mean intensities, we obtain the following expressions.

$$\begin{aligned} \Gamma(u, u) &= \frac{1}{A_u A_u} \oint_{\vec{C}} (I - u)(I - u) ds \\ \Gamma(u, v) &= \frac{-1}{A_u A_v} \oint_{\vec{C}} (I - u)(I - v) ds \\ \Gamma(v, v) &= \frac{1}{A_v A_v} \oint_{\vec{C}} (I - v)(I - v) ds \end{aligned}$$

The constraint that  $u$  and  $v$  must move in opposite directions is equivalent to  $u'v' < 0$ , which, using equations (12) and (13), leads to the following condition.

$$\Gamma(u, v)(\Gamma(u, u) + \Gamma(v, v)) < \Gamma(u, u)\Gamma(v, v) + \Gamma^2(u, v) \quad (14)$$

We enforce this constraint by using the unconstrained binary flow  $-\nabla E$  so long as (14) is satisfied. If this condition is not satisfied, we modify the evolution to keep either  $u$  or  $v$  fixed (depending upon which one is moving in the “wrong” direction) by removing the component along the gradient direction for that statistic. We therefore choose one of the following con-

<sup>3</sup>i.e. the flows which increase  $u$  and  $v$  most quickly, see (2)

strained binary flows,

$$\frac{d\vec{C}}{dt} = -\nabla E + \frac{\langle \nabla E, \nabla u \rangle}{\langle \nabla u, \nabla u \rangle} \nabla u = \frac{u - v}{A_v} ((I - u) + \gamma_u (I - v)) \vec{N} \quad (15)$$

$$\frac{d\vec{C}}{dt} = -\nabla E + \frac{\langle \nabla E, \nabla v \rangle}{\langle \nabla v, \nabla v \rangle} \nabla v = \frac{u - v}{A_u} ((I - v) + \gamma_v (I - u)) \vec{N} \quad (16)$$

where flow (15) is used to preserve the value of  $u$ , while flow (16) is used to preserve the  $v$  value of  $v$ , and where

$$\gamma_u = \frac{\oint_{\vec{C}} (I - u)(I - v) ds}{\oint_{\vec{C}} (I - u)(I - u) ds} \quad \text{and} \quad \gamma_v = \frac{\oint_{\vec{C}} (I - u)(I - v) ds}{\oint_{\vec{C}} (I - v)(I - v) ds}.$$

In the bottom row of Fig. 2 we see this new constrained flow remedying the poor performance of the original, unconstrained flow (5). With the constraints, the final contour remains along the boundary of the ventricle instead of collapsing into the blood pool.

### 3.2 A more general constraint

For the binary flow, we considered the constraint that the two statistics  $u$  and  $v$  must move in opposite directions. This viewpoint is difficult to generalize to models, such as the ternary model, which involve more than two statistics. However, if we view the binary constraint in a slightly different light, i.e. we want the statistic  $u$  to evolve in such a way that if the other statistic  $v$  were held fixed, the distance between  $u$  and  $v$  would still increase (and vice-versa) then we create a perspective that carries over naturally when more

than two statistics are involved. The constraint, in the general multimodal case involving  $n - 1$  coupled curve evolution equations, is that each statistic must evolve in a direction that would increase the volume of the  $n - 1$  dimensional simplex whose vertices are given by the values of  $n$  statistics (see Section 2.3). An equivalent geometric statement is that each vertex must move away from the opposite face of the simplex.

### 3.3 Constrained ternary flows

Here we apply the general constraint, dictated above, to our ternary model, which involves three statistics  $u$ ,  $v$ , and  $w$ . In this case, the constraint is that  $u'$  (the time derivative of  $u$ ) must be directed away from the line segment connecting  $v$  and  $w$  (as to increase the area of the triangle  $T_{uvw}$  if  $v$  and  $w$  were held fixed). We employ similar constraints for  $v'$  and  $w'$  and will make these conditions more precise shortly. First we derive expressions for  $u'$ ,  $v'$ , and  $w'$ .

If  $\theta_i$  denotes the  $i$ 'th component of one of the  $n$ -dimensional statistics  $u$ ,  $v$ , or  $w$ , its time derivative  $\theta'_i$  under the coupled flows  $-\nabla_{\vec{C}_u} E$  and  $-\nabla_{\vec{C}_v} E$  given by (9) and (10) may be computed as

$$\theta'_i = \theta_i'^u + \theta_i'^v = -\langle \nabla_{\vec{C}_u} \theta_i, \nabla_{\vec{C}_u} E \rangle - \langle \nabla_{\vec{C}_v} \theta_i, \nabla_{\vec{C}_v} E \rangle$$

where  $\theta_i'^u$  and  $\theta_i'^v$  denote the derivatives of  $\theta_i$  strictly due to the evolutions of  $\vec{C}_u$  and  $\vec{C}_v$  respectively. If we ignore the arclength terms in (8), and therefore the corresponding curvature terms in (9) and (10),

$$\begin{aligned} \theta_i'^u &= \sum_{j=1}^n \langle \nabla_{\vec{C}_u} \theta_i, \bar{w}_j \nabla_{\vec{C}_u} u_j + \bar{v}_j \nabla_{\vec{C}_u} w_j \rangle \\ \theta_i'^v &= \sum_{j=1}^n \langle \nabla_{\vec{C}_v} \theta_i, \bar{u}_j \nabla_{\vec{C}_v} v_j + \bar{w}_j \nabla_{\vec{C}_v} w_j \rangle \end{aligned}$$

we obtain the following expressions,

$$\begin{aligned} u'^u &= \Gamma_{\vec{C}_u}(u, u) \bar{w} + \Gamma_{\vec{C}_u}(u, w) \bar{v} & v'^v &= \Gamma_{\vec{C}_v}(v, v) \bar{u} + \Gamma_{\vec{C}_v}(v, w) \bar{w} \\ w'^u &= \Gamma_{\vec{C}_u}(w, u) \bar{w} + \Gamma_{\vec{C}_u}(w, w) \bar{v} & w'^v &= \Gamma_{\vec{C}_v}(w, v) \bar{u} + \Gamma_{\vec{C}_v}(w, w) \bar{w} \end{aligned}$$

where  $\Gamma_{\vec{C}_u}$  and  $\Gamma_{\vec{C}_v}$  denote matrices of inner products of gradient flows, with respect to  $\vec{C}_u$  and  $\vec{C}_v$  respectively, for the components of the two statistics passed as arguments. For example, the entry  $\Gamma_{\vec{C}_u}^{ij}(u, w)$  in the  $i$ 'th row and  $j$ 'th column of  $\Gamma_{\vec{C}_u}(u, w)$  would be given by  $\langle \nabla_{\vec{C}_u} u_i, \nabla_{\vec{C}_u} w_j \rangle$ . In the case that  $u$ ,  $v$ , and  $w$  represent means of a vector-valued image  $I = (I_1, \dots, I_n)$ ,

$$\begin{aligned} \Gamma_{\vec{C}_u}(u, u) &= \frac{1}{A_u A_u} \oint_{\vec{C}_u} (I - u)(I - u)^T ds \\ \Gamma_{\vec{C}_u}(u, w) &= \frac{1}{A_u A_w} \oint_{\vec{C}_u} (I - u)(I - w)^T (1 - \chi_u) ds \\ \Gamma_{\vec{C}_u}(w, w) &= \frac{1}{A_w A_w} \oint_{\vec{C}_u} (I - w)(I - w)^T (1 - \chi_u) ds \end{aligned}$$

and

$$\begin{aligned} \Gamma_{\vec{C}_v}(v, v) &= \frac{1}{A_v A_v} \oint_{\vec{C}_v} (I - v)(I - v)^T ds \\ \Gamma_{\vec{C}_v}(v, w) &= \frac{1}{A_v A_w} \oint_{\vec{C}_v} (I - v)(I - w)^T (1 - \chi_u) ds \\ \Gamma_{\vec{C}_v}(w, w) &= \frac{1}{A_w A_w} \oint_{\vec{C}_v} (I - w)(I - w)^T (1 - \chi_u) ds \end{aligned}$$

(the other two matrices  $\Gamma_{\vec{C}_u}(w, u)$  and  $\Gamma_{\vec{C}_v}(w, v)$ , are transposes of  $\Gamma_{\vec{C}_u}(u, w)$  and  $\Gamma_{\vec{C}_v}(v, w)$  respectively).

We now state our constraints more precisely as

$$u' \cdot h^u > 0, \quad v' \cdot h^v > 0, \quad w' \cdot h^w > 0 \quad (17)$$

where

$$u' = u'^u, \quad v' = v'^v, \quad w' = w'^u + w'^v$$

and where  $h^u$ ,  $h^v$ , and  $h^w$  denote vectors perpendicular to the edges of the triangle  $T_{uvw}$  opposite the vertices  $u$ ,  $v$ , and  $w$  (represented by the vectors  $(v - w)$ ,  $(w - u)$ , and  $(u - v)$  respectively) and directed toward the interior of the triangle (when starting from any point on the respective edges of  $T_{uvw}$ ). The following vectors constitute such a set.

$$\begin{aligned} h^u &= u(\hat{v} \cdot \hat{v}) + v(\hat{v} \cdot \hat{w}) + w(\hat{v} \cdot \hat{u}) \\ h^v &= v(\hat{w} \cdot \hat{w}) + u(\hat{w} \cdot \hat{u}) + u(\hat{w} \cdot \hat{v}) \\ h^w &= w(\hat{u} \cdot \hat{u}) + u(\hat{u} \cdot \hat{v}) + v(\hat{u} \cdot \hat{w}) \end{aligned} \quad (18)$$

We enforce these constraints as follows. We start out, as we did in the binary case, by using the unconstrained flows  $-\nabla_{\vec{C}_u} E$  and  $-\nabla_{\vec{C}_v} E$  given by (9) and (10) as long as the conditions in (17) are satisfied. If these conditions are not satisfied, we use one or more of the following constrained ternary flows which restrict the motion of each problematic statistic so that its distance from the opposite edge of the triangle  $T_{uvw}$  remains fixed (when ignoring the evolution of the other two statistics) and therefore does not change the value of the cost functional  $E$  (if the arclength penalties are ignored).

$$\frac{d\vec{C}_u}{dt} = -\nabla_{\vec{C}_u} E + \begin{cases} \gamma_u^u \nabla_{\vec{C}_u} (u \cdot h^u), & u'^u \cdot h^u < 0 \\ \gamma_w^u \nabla_{\vec{C}_u} (w \cdot h^w), & w'^u \cdot h^w < 0 \end{cases} \quad (19)$$

$$\frac{d\vec{C}_v}{dt} = -\nabla_{\vec{C}_v} E + \begin{cases} \gamma_v^v \nabla_{\vec{C}_v} (v \cdot h^v), & v'^v \cdot h^v < 0 \\ \gamma_w^v \nabla_{\vec{C}_v} (w \cdot h^w), & w'^v \cdot h^w < 0 \end{cases} \quad (20)$$

The following expressions pertain to (19) and (20).

$$\begin{aligned} \gamma_u^u &= \frac{\langle \nabla_{\vec{C}_u} (u \cdot h^u), \nabla_{\vec{C}_u} E \rangle}{\langle \nabla_{\vec{C}_u} (u \cdot h^u), \nabla_{\vec{C}_u} (u \cdot h^u) \rangle} = \frac{h^u \cdot u'^u}{h^u \cdot \Gamma_{\vec{C}_u}(u, u) h^u} \\ \gamma_w^u &= \frac{\langle \nabla_{\vec{C}_u} (w \cdot h^w), \nabla_{\vec{C}_u} E \rangle}{\langle \nabla_{\vec{C}_u} (w \cdot h^w), \nabla_{\vec{C}_u} (w \cdot h^w) \rangle} = \frac{h^w \cdot w'^u}{h^w \cdot \Gamma_{\vec{C}_u}(w, w) h^w} \end{aligned}$$

$$\gamma_v^v = \frac{\langle \nabla_{\vec{C}_v}(v \cdot h^v), \nabla_{\vec{C}_v} E \rangle}{\langle \nabla_{\vec{C}_v}(v \cdot h^v), \nabla_{\vec{C}_v}(v \cdot h^v) \rangle} = \frac{h^v \cdot v^v}{h^v \cdot \Gamma_{\vec{C}_v}(v, v) h^v}$$

$$\gamma_w^v = \frac{\langle \nabla_{\vec{C}_v}(w \cdot h^w), \nabla_{\vec{C}_v} E \rangle}{\langle \nabla_{\vec{C}_v}(w \cdot h^w), \nabla_{\vec{C}_v}(w \cdot h^w) \rangle} = \frac{h^w \cdot w^v}{h^w \cdot \Gamma_{\vec{C}_v}(w, w) h^w}$$

$$\nabla_{\vec{C}_u}(u \cdot h^u) = \sum_{i=1}^n h_i^u \nabla_{\vec{C}_u} u_i = \sum_{i=1}^n h_i^u \frac{I_i - u_i}{A_u} \vec{N}_u$$

$$\nabla_{\vec{C}_u}(w \cdot h^w) = \sum_{i=1}^n h_i^w \nabla_{\vec{C}_u} w_i = -(1 - \chi_v) \sum_{i=1}^n h_i^w \frac{I_i - w_i}{A_w} \vec{N}_u$$

$$\nabla_{\vec{C}_v}(v \cdot h^v) = \sum_{i=1}^n h_i^v \nabla_{\vec{C}_v} v_i = \sum_{i=1}^n h_i^v \frac{I_i - v_i}{A_v} \vec{N}_v$$

$$\nabla_{\vec{C}_v}(w \cdot h^w) = \sum_{i=1}^n h_i^w \nabla_{\vec{C}_v} w_i = -(1 - \chi_u) \sum_{i=1}^n h_i^w \frac{I_i - w_i}{A_w} \vec{N}_v$$

## 4 Results

We now present some additional medical images which cannot be segmented using the original binary or ternary flows but require instead the constrained versions presented in the previous section. In each case we start with the same initial contour and show snapshots of both the constrained and unconstrained flows at identical times during the evolution process.

In the bottom row of Fig. 3 we observe the constrained binary flow (15-16) segmenting the white matter in a MRI brain image; while in the top row, we see the original binary flow (5) capturing only a tiny bright spot inside. In the bottom row of Fig. 4 we observe the constrained binary flow (15-16) segmenting the left ventricle in a cardiac MRI image; while in the top row, the original binary flow (5) once again captures only a few bright pixels inside. Finally, in Fig. 5 we demonstrate the constrained ternary flows (19) and (20) distinguishing three regions in a color image of the skin surface on the hand of a patient with a Kaposi Sarcoma. Both flows capture the background region successfully. However, only the constrained version (bottom row) captures the lesion whereas the unconstrained version (top row) collapses inside the lesion.

## 5 Conclusions

In conclusion, we have outlined a fully global approach to segmentation based upon curve evolution models designed to separate two or more values of a given set of statistics. By dictating that the statistics must also move "away from each other," we obtained a global constraint which greatly improved the performance of the original model, allowing us to segment a number of images for which the original, unconstrained model would fail.

## References

- [1] A. Chakraborty, L. Staib, and J. Duncan, "Deformable Boundary Finding in Medical Images by Integrating Gradient and Region Information," *IEEE Trans. Medical Imaging*, **15:6**, pp. 859–870, Dec. 1996.
- [2] T. Chan and L. Vese, "Active contours without edges," UCLA Technical Report submitted to *IEEE Trans. Image Processing* 1999.
- [3] M. Kass, A. Witkin, and D. Terzopoulos, "Snakes: active contour models," *Int. Journal of Computer Vision*, **1**, pp. 321–331, 1987.
- [4] R. Malladi, J. Sethian, and B. Vemuri, "Shape modeling with front propagation: a level set approach," *IEEE Trans. Pattern Anal. Machine Intell.*, **17**, pp. 158–175, 1995.
- [5] D. Mumford and J. Shah, "Optimal approximations by piecewise smooth functions and associated variational problems," *Communications in Pure and Applied Mathematics*, **42:4**, 1989.
- [6] S. Osher and J. Sethian, "Front propagation with curvature dependent speed: Algorithms based on Hamilton-Jacobi formulations," *Journal of Computational Physics*, **79**, pp. 12–49, 1988.
- [7] N. Paragios and R. Deriche, "Geodesic Active Regions for Texture Segmentation," Research Report 3440, INRIA, France, 1998.
- [8] R. Ronfard, "Region-Based Strategies for Active Contour Models," *Int. J. Computer Vision*, **13:2**, pp. 229–251, 1994.
- [9] J. Sethian, *Level Set Methods*, Cambridge University Press, 1996.
- [10] A. Yezzi, A. Tsai, and A. Willsky, "Fully Global, Coupled Curve Evolution Equations for Image Segmentation," LIDS Technical Report, January, 1999 (submitted to *IEEE Trans. on PAMI*).
- [11] A. Yezzi, A. Tsai, and A. Willsky, "A Statistical Approach to Image Segmentation for Bimodal and Trimodal Imagery," *Proceedings of ICCV*, September, 1999.
- [12] S. Zhu and A. Yuille, "Region Competition: Unifying snakes, Region Growing, and Bayes/MDL for Multiband Image Segmentation," *IEEE Trans. Pattern Anal. Machine Intell.*, **18:9**, pp. 884–900, Sep. 1996.

Figure 3: Constrained (bottom) and unconstrained (top) binary flows applied to an MRI brain image.

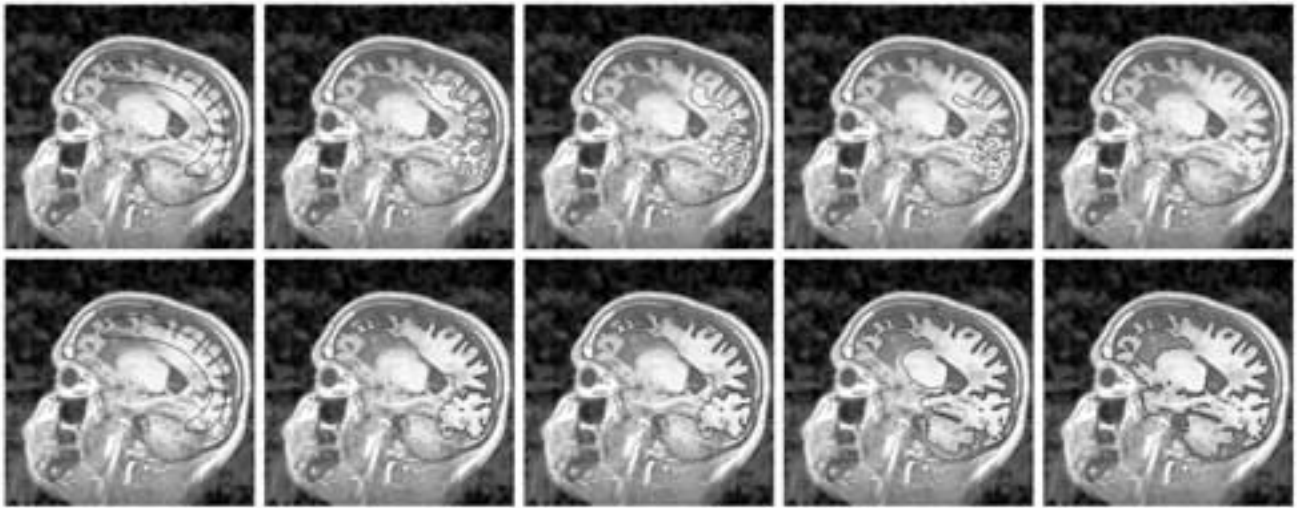


Figure 4: Constrained (bottom) and unconstrained (top) binary flows applied to a cardiac MRI image.

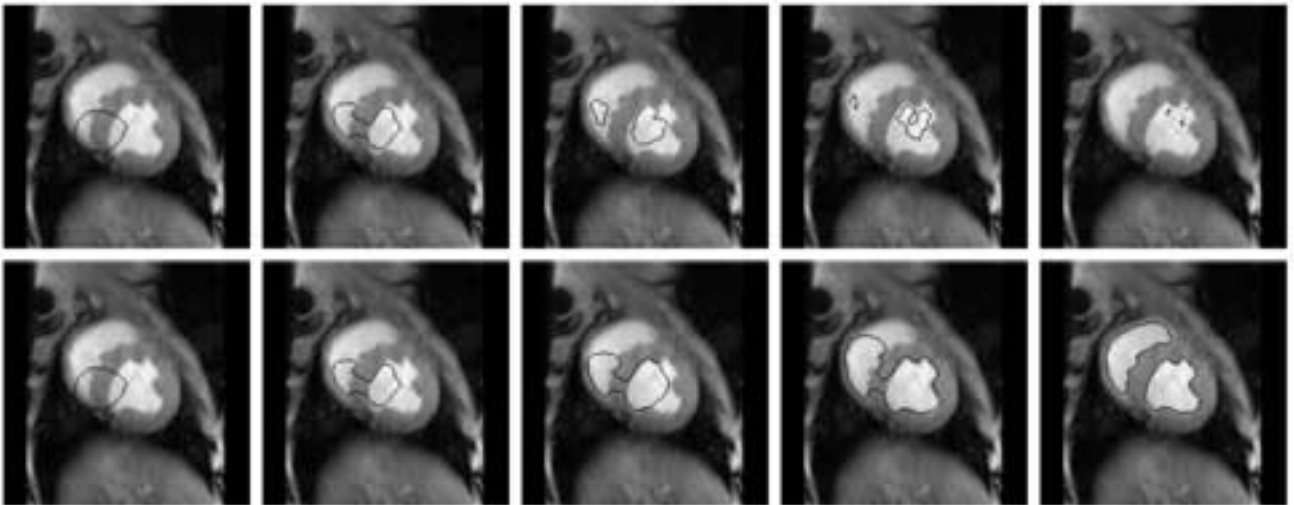


Figure 5: Constrained (bottom) and unconstrained (top) ternary flows applied to a skin surface image.

